A Study of Near to Far Fields of JPL Deep Space Network (DSN) Antennas for RFI Analysis[1,2]

Vahraz Jamnejad
Jet Propulsion Laboratory
California Institute of Technology
Pasadena, CA 91109
818-354-2674
vahraz.jamnejad@jpl.nasa.gov

Abstract— This paper addresses the issue of calculating the gain and power distribution of DSN antennas in the Fresnel (middle zone) and Fraunhofer (far zone) as a function of the distance from the DSN antenna and the off-boresight angle. Calculating the near and mid fields of DSN antennas are of interest in the receive mode where the transmitting signals from nearby flying objects such as helicopters and airplanes transmitting in the DSN frequency range, interfere with the operation of sensitive RF receiving system of the DSN antennas, and in the transmit mode where fields from high-powered DSN antennas interfere with receivers on nearby flying objects such as helicopters or other systems. Computing the exact fields of a large DSN antenna is, in general, a very complicated and arduous task. Even far-field calculations, which are less complicated compared to near and mid zone fields, take considerable computer time. These calculations become even more involved and time-consuming in very near field and back field regions. We provide two approaches for addressing the radio frequency interference (RFI) issue. In this paper actual fields in mid and far zones are calculated using a relatively simple formulation that is accurate enough for the purposes of RFI analysis. In a future paper we will study and develop simple reference models that provide upper limit bounds or envelopes of the far field patterns as a function of the antenna diameter and frequency, which can be used for obtaining the field at any given point in space.

TABLE OF CONTENTS

1. INTRODUCTION 1
2. FORMULATION OF THE PROBLEM 2
4. NUMERICAL RESULTS 6
5. SUMMARY AND CONCLUSIONS 6
ACKNOWLEDGMENT 6
REFERENCES 6
BIOGRAPHY 6

1. INTRODUCTION

Calculating the mid and near field of DSN antennas are of interest in two general situations:

1- Receive mode: When the transmitting signals from nearby flying objects such as helicopters and airplanes or other systems which transmit in the DSN frequency range, interfere with the operation of the DSN antenna systems in a the receiving mode.

2- Transmit mode: When the transmitted fields from high-powered DSN antennas interfere with sensitive RF receiving systems on nearby flying objects such as helicopters and airplanes or other systems with critical radio frequency requirements.

Table 1 summarizes the various DSN antennas of interest with the applicable frequencies and transmitted power capabilities. But computing the exact fields of a large DSN antenna is, in general, a very complicated and arduous task. Even far-field calculations which are relatively easier compared to the near and middle zone region, take from minutes to hours on a CRAY computer depending on the frequency of interest. These calculations become even more involved and time-consuming in the near field and back field regions.

Furthermore, there are many factors that cannot be completely taken care of in an easy manner, such as surface errors, mis-alignments, and wind and gravity effects. And many of these parameters change in time and for various azimuth and elevation angles.

Two complementary methods are pursued in addressing the radio frequency interference (RFI) issue.

i- In this paper actual fields in mid and far zones are

[1] 0-7803-8155-6/04/$17.00© 2004 IEEE
[2] IEEEAC paper #1546, Final Version, Updated December 15, 2003

calculated using a relatively simple formulation that is accurate enough for the purposes of RFI analysis.

ii- In a future paper we provide simple reference models for the upper limit or envelope of the near and far field patterns as functions of the antenna diameter and frequency which can be used for obtaining the field at any given point in space

2. FORMULATION OF THE PROBLEM

Geometry of the problem

As shown in Figure 1, the orientation of the DSN antenna towards a spacecraft is specified by two parameters: the azimuth angle, ϕ_s , and the elevation angle, γ_s , of the boresight direction.

The position of the observation point, namely the location of the interfering object is given by its azimuth, ϕ, its vertical height from the ground, h, and its distance from the base of the DSN antenna, l. These parameters are used to calculate the elevation angle of the observation point, γ, and the distance from the ground antenna to the observation points, r, as given below.

$$\beta = \frac{l}{R} \tag{1}$$

$$\tan(\gamma) = \frac{\cos(\beta) - \dfrac{1}{1+\frac{h}{R}}}{\sin(\beta)} \tag{2}$$

$$\sin(\alpha) = \frac{\cos(\gamma)}{1+\frac{h}{R}} \tag{3}$$

$$r = R(1+\frac{h}{R})\frac{\sin(\beta)}{\cos(\gamma)} = R\frac{\sin(\beta)}{\sin(\alpha)} \tag{4}$$

Once the azimuth and elevation angles of the boresight direction and the observation point directions are known, the angle, θ, between these two directions is obtained such that

$$\cos(\theta) = \sin(\gamma_s)\sin(\gamma) + \cos(\gamma_s)\cos(\gamma)\cos(\phi) \tag{5}$$

The polar angle θ and the distance r in the antenna coordinate system are the only parameters needed to obtain the field information at any given point, assuming that the field pattern is circularly symmetric, which is an acceptable assumption for the purpose of this study.

An approximate field for the antenna at any observation point, with two parameters of distance and angle from boresight, is obtained using a relatively simple scalar formulation, which can be used for obtaining the mid-field and far-field with a reasonable degree of accuracy. But first we define the various field regions.

Field region definition

Based on the characteristics of the radiated field from the aperture antennas, their dependence on various parameters and the level of difficulty in their calculations, three regions or zones of radiation are customarily distinguished:

Near field region This region is also referred to as the induction field region, where the field has a very complicated behavior, and its calculation requires the calculation of the radiation integral in its most general form. Any reasonable computation would require substantial amount of computer time, and even so it is highly dependent on various irregularities and deformities of the antenna structure. If needed and possible, the measurement is perhaps the best way of obtaining meaningful results. Depending on the size of the "effective" aperture of the antenna, D, the boundaries of this region in terms of the distance from the aperture, d, varies.

Mid field or Fresnel region This is the region from near zone to the far zone or field region starting at 2 D^2/λ. This is basically a transition region between the near field and the far field region. The criterion used to establish the boundary between near and Fresnel zone is that the difference in parameter (1/r) exp($j2\pi r/\lambda$) does not exceed $\pi/8$ radians in phase (equivalent to $\lambda/16$ in path length), and $\lambda/16$ in amplitude, at any point in space from any two points over the aperture (r being the distance between the point in space and the point on the aperture)[1].

Far field or Fraunhofer region This is the region from 2 D2/λ to infinity, where the antenna field has a 1/r dependency on distance from the antenna center and a very nearly spherical phase front. The boundary between the far or Fraunhofer field and the middle or Fresnel field is taken to be such that their be no greater phase difference than ($\pi/8$) radians (or $\lambda/16$ path length difference) at a point in space from any two points in the aperture [1]. This condition results in the $2D^2/\lambda$ criterion and leads to certain simplifications in the radiation integral.

These boundaries are calculated and summarized below as:

i- for $D/\lambda < 1$,

near field: $d/D < 1/(D/\lambda)$
or $d/\lambda < 1$ (6)

far field: $d/\lambda > 1/(D/\lambda)$
or $d/\lambda > 1$ (7)

ii- for $1<D/\lambda<10$,

near field: $d/D < 0.5/\tan(\pi/8)=1.2$
or $d/\lambda < 1.2\ (D/\lambda)$ (8)

mid field: $1.2 < d/D < 2(D/\lambda)$
or $1.2\,(D/\lambda) < d/\lambda < 2(D/\lambda)^2$ (9)

far field: $d/D > 2(D/\lambda)$
or $d/\lambda > 2(D/\lambda)^2$ (10)

iii- for $D/\lambda > 10$,

near field: $d/D < \frac{1}{2}(D/\lambda)^{1/3}$
or $d/\lambda < \frac{1}{2}(D/\lambda)^{4/3}$ (11)

mid field: $0.5(D/\lambda)^{1/3} < d/D < 2/(D/\lambda)$
or $0.5(D/\lambda)^{4/3} < d/\lambda < 2(D/\lambda)^2$ (12)

far field: $d/D > 2(D/\lambda)$
or $d/\lambda > 2(D/\lambda)^2$ (13)

For typical reflector antennas the diameter is more than 10 wavelengths and therefore only the condition iii is of interest. Graphical plots of the various regions are given in Figure 2. Table 2 provides the mid (Fresnel) and far (Fraunhofer) zone limits for the DSN antennas of interest at various operational frequencies.

Field calculations

The following assumptions are made in obtaining the fields.

1- The pattern is circularly symmetric

2- A scalar formulation for the field is used. The actual field is of a vectorial nature, but for simplicity of calculations we use a scalar formulation.

3- The field on the aperture is assumed to be uniform in amplitude. This is approximately valid, since the reflector system is shaped to produce a uniform phase and a fairly uniform amplitude distribution on the aperture with drop-off at the edges to reduce diffraction. Assuming uniformity to the edge actually gives a more pessimistic result for the sidelobes, which is acceptable here.

4- The field on the aperture is assumed to be uniform in phase. The reflector is designed to produce uniform phase on the aperture. However, the surface errors, mis-alignments, gravity and wind pressure effects will distort this uniform phase front. For the purpose of this study we ignore these effects. Although, they can be included at a later stage.

5- The Fresnel approximation is made to the exponential kernel in the radiation integral. Namely, the distance from the observation point to a point on the aperture, r, is approximated by a linear term of the normal distance to the aperture and a quadratic term of distance from the central axis. This is equivalent to a phase difference less than ($\pi/8$) or ($\lambda/16$) at a point in space from any point in the aperture as discussed above [1].

Based on these assumptions the fields can be obtained in the following forms. These forms are based on the formulations given in [2] and [3], but are in a slightly different presentation. Figure 3 shows a 2-D view of the antenna aperture and the various zones for calculation.

First the following parameters are first defined:

Parameter Definitions

λ, wavelength
D, aperture diameter
$R = D/2$, aperture radius
r, distance from observation point to the origin at the center of aperture
θ, angle between observation direction and main axis
$d = r\cos(\theta)$, normal distance to the aperture from an observation point
$\rho = r\sin(\theta)$, normal distance from observation point to the main axis
$R_n = R/\sqrt{(\lambda d/\pi)}$, normalized R
$\rho_n = \rho/\sqrt{(\lambda d/\pi)}$, normalized ρ
E_0 = constant (or average) electric field on the aperture
$E(r, \theta)$ = electric field at the observation point
$G = (4\pi r^2)\,(E(r, \theta)^2) / (\pi R^2 E_0^2) = 4\,(r/R)^2\,(E(r, \theta)/E0)^2$, definition of directivity
$G_0 = (\pi D/\lambda)^2$, maximum peak directivity
$\mathrm{Sinc}[x] = \sin[x]/x$, the sinc or sampling function
$\Lambda_n[x] = (n!)\,J_n[x] / (x/2)^n$, Lambda function or normalized Bessel function

Now, given the constant (or average) field distribution, E_0, on the aperture, the field $E(r, \theta)$ is first calculated. Subsequently the directivity $G(r, \theta)$ is obtained. The gain then would be obtained by simply multiplying the directivity by an efficiency factor η. However, here we use the symbol G to loosely describe both directivity and gain, but the meaning should be understood in context. Notice that with this definition, the gain is, in general, a function of both r and θ. Only in the far field where the E field has a 1/r dependence, the gain becomes solely a function of polar angle θ. In summary, the gain functions in different regions defined in Figure 3 are given as follows.

I) In the vicinity of the main axis such that ρ<R,

$$G(r,\theta)=(\frac{\pi D}{\lambda})^2(\frac{1+\cos(\theta)}{2\cos(\theta)})^2\frac{1}{(R_n^{\ 2})^2}\left\{\begin{array}{l}\left[\sin^2[R_n^{\ 2}+\rho_n^{\ 2}]-\sum_{n=0}^{\infty}(-1)^n\frac{(\rho_n^{\ 2})^{2n+1}}{(2n+1)!}\Lambda_{2n+1}[(\frac{\pi D}{\lambda})\tan(\theta)]\right]^2+\\ \left[\cos^2[R_n^{\ 2}+\rho_n^{\ 2}]-\Lambda_0[(\frac{\pi D}{\lambda})\tan(\theta)]+\sum_{n=0}^{\infty}(-1)^n\frac{(\rho_n^{\ 2})^{2n+2}}{(2n+2)!}\Lambda_{2n+2}[(\frac{\pi D}{\lambda})\tan(\theta)]\right]^2\end{array}\right\} \quad (14)$$

II) In the region away from axis, ρ> R,

$$G(r,\theta)=(\frac{\pi D}{\lambda})^2(\frac{1+\cos(\theta)}{2\cos(\theta)})^2\frac{1}{(R_n^{\ 2})^2}\left\{\begin{array}{l}\left[\sum_{n=0}^{\infty}(-1)^n\frac{(R_n^{\ 2})^{2n+1}}{(2n+1)!}\Lambda_{2n+1}[(\frac{\pi D}{\lambda})\tan(\theta)]\right]^2+\\ \left[\sum_{n=0}^{\infty}(-1)^n\frac{(R_n^{\ 2})^{2n+2}}{(2n+2)!}\Lambda_{2n+2}[(\frac{\pi D}{\lambda})\tan(\theta)]\right]^2\end{array}\right\} \quad (15)$$

III) In the far field region, R_n <<1 or d >> $\pi R^2/\lambda$

$$G(\theta)=(\frac{\pi D}{\lambda})^2(\frac{1+\cos(\theta)}{2\cos(\theta)})^2\Lambda_1^{\ 2}[(\frac{\pi D}{\lambda})\tan(\theta)] \quad (16)$$

Notice that this last expression is a function of angle θ only.

IV) On the boresight axis of the antenna,

$$G(r)=(\frac{\pi D}{\lambda})^2\sin c^2(\frac{\pi}{8}\frac{D^2}{d\lambda}),\ for\ \rho=\theta=0 \quad (17)$$

Notice that this last expression has zeros (minima) at

$$\frac{\pi}{8}\frac{D^2}{d\lambda}=n(\frac{\pi}{2}),\ n=2,4,6,...\theta$$
$$or \quad (18)$$
$$d=\frac{1}{8n}(\frac{2D^2}{\lambda}),\ n=2,4,6,...$$

and maxima at

$$\frac{\pi}{8}\frac{D^2}{d\lambda}=n(\frac{\pi}{2}),n=1,3,5,...$$
$$or \quad (19)$$
$$d=\frac{1}{8n}(\frac{2D^2}{\lambda})$$

For decreasing values of d, the function has a linear envelope given by

$$G(d)=(\frac{\pi D}{\lambda})^2(\frac{8d\lambda}{\pi D^2})^2=(\frac{8d}{D})^2,\ for\ d\le\frac{\pi D^2}{8\lambda} \quad (20)$$

As already mentioned, since the above formulas start from the aperture and do not include any losses prior to the aperture, they basically represent directivity. An efficiency number η must be included to account for feed spillover, polarization and other losses, in order to obtain the gain.

Gain and power density relationships

A different but sometimes more useful parameter is the power density at each field point. Consider a transmitting antenna with a total transmitted power P_t and an aperture area $A=\pi D^2/4$ in which D is the diameter of the aperture. Furthermore assume that the field distribution on the aperture is uniform with an average value of

$$p_a=\frac{P_t}{A}=\frac{4P_t}{\pi D^2} \quad (21)$$

The directive gain of this antenna, which is an indication of the angular variation of the power distribution, is defined by

$$G_t(\theta,\phi)=\frac{4\pi\ p(\theta,\phi)}{P_t} \quad (22)$$

in which $p(\theta,\phi)$ is the angular power flux density (power per unit steradian) of the outgoing field. By definition, the gain depends only on angle and is independent of the radial distance. The definition of gain, however, can be extended to a radial-dependent case by defining

$$G_t(r,\theta,\phi)=\frac{4\pi r^2\ p_d(r,\theta,\phi)}{P_t} \quad (23)$$

in which $p_d(r,\theta,\phi)$ is the power flux density per unit of area. This is a valid expression for the near and mid-field regions where the outgoing field can still be assumed to be outgoing and the poynting vector is in the radial direction. For the very near field region, the poynting vector may not be radial and indeed it may not be outgoing at all, and all sorts of complications and polarization non-uniformities exist and the dependence on r is of a much higher order. However, in the far field distance from the antenna p_d is related to p by

$$p_d(r,\theta,\phi) = \frac{1}{r^2} p(\theta,\phi) \tag{24}$$

Namely, field dependence on the distance is of the form $1/r$. In this case the r dependence drops out from the expression for gain and latter r-dependent expression for gain reduces to the former standard expression for the angular gain.

The peak gain is given by

$$G_{\max} = \eta \frac{4\pi}{\lambda^2} A = \eta(\pi D/\lambda)^2 \tag{25}$$

and conversely

$$A = \frac{1}{\eta}\frac{\lambda^2}{4\pi} G_{\max} \tag{26}$$

In which η, as mentioned before, is the efficiency which accounts for feed spillover, polarization and other losses prior to the aperture.

Using the radial-dependent form of the gain we can write the power density as

$$p_d(r,\theta,\phi) = \frac{P_t G_t(r,\theta,\phi)}{4\pi r^2} = \frac{EIRP}{4\pi r^2} \tag{27}$$

in which $EIRP$ is the *effective isotropically radiated power* given as

$$EIRP = P_t G_t(r,\theta,\phi) \tag{28}$$

The received power by an aperture antenna with an effective aperture of A_r is then given as

$$P_r = p_d A_r \tag{29}$$

or

$$P_r = \frac{P_t G_t}{4\pi r^2} A_r = \frac{P_t G_t}{4\pi r^2}\frac{\lambda^2}{4\pi} G_{r\max} \tag{30}$$

or finally,

$$P_r == P_t G_t G_{r\max} \frac{1}{(4\pi r/\lambda)^2} = P_t G_t G_{r\max} / L_s \tag{31}$$

in which space loss is defined as

$$L_s = (4\pi r/\lambda)^2 \tag{32}$$

This is the well-known Friis transmission formula used in standard link budget calculations.

Normalization of the power density and gain

In some cases it is convenient to use a normalized form of the power density and gain. The power density can be normalized with respect to the average power density on the aperture as follows.

$$p_{dn} = p_d / p_a = (\frac{P_t G}{4\pi r^2})/(\frac{P_t}{A}) = \frac{A}{4\pi r^2} G \tag{33}$$

Similarly, the gain can be normalized to peak gain as

$$G_n = G / G_{\max} \tag{34}$$

The normalized power density is then related to the normalized gain as

$$p_{dn} = \frac{A_t}{4\pi r^2} G_n G_{\max} = \frac{A_t}{4\pi r^2}\frac{4\pi}{\lambda^2} A_t G_n = \frac{A_t^2}{r^2\lambda^2} G_n \tag{35}$$

or

$$p_{dn} = \left(\frac{\pi D^2}{4r\lambda}\right)^2 G_n \tag{36}$$

Let's define a normalized radial distance from the aperture as

$$r_n = \frac{4r\lambda}{D^2} = \frac{r}{r_c} \tag{37}$$

in which $r_c = \dfrac{D^2}{4\lambda}$ is a characteristic radius defining the location of the last peak of the power density along the aperture and the onset of the far field region (The far field is actually defined as starting at 8 r_c.

Then, the normalized power density and gain are related as

$$p_{dn} = (\frac{\pi}{r_n})^2 G_n \tag{38}$$

4. NUMERICAL RESULTS

All the above formulas have been programmed into a MATLAB to obtain the gain and power density at any (r, θ) observation point. A few sample figures using the program are given below.

Figure 4 shows the variation of gain along the main axis (boresight direction) of the antenna. Figure 5 presents a similar plot for the normalized power density. The positions of the minima (zeros) and maxima are clearly observed in both figures. As can be seen, starting from near the aperture the field is highly oscillatory going through a set of minima (zeros) and maxima with a simple linear envelope for the gain (in dB) and a constant envelope for the power density. In approaching the far field region the gain reaches a constant value while power density has a linear envelope.

Figure 6 shows the gain on various spheres away from the aperture center as a function of $\tan(\theta)/(0.5D/\lambda)$ which is an indication of the angle off boresight normalized to approximately half the 3-dB beamwidth.

Figure 7 shows the gain and power density on various planes with fixed distances from aperture center, as a function of distance from the center axis. Figure 8 presents a similar plot for the power density. Notice that on the planes near the aperture, the field becomes nearly constant with minor oscillations in the aperture region and falls to half power (6 dB) at the edge. Figure 9 provides a 3-D plot of the normalized power density, p_n, versus the normalized distance from the boresight axis, $x = \rho / R = 2\, d \tan(\theta) / D$, and the normalized distance from the aperture $n = 4\, d\, \lambda/D^2$, as coordinates. Figures 10 and 11 show color contour plots of the normalized power density with the same coordinates.

5. SUMMARY AND CONCLUSIONS

In this study we have formulated the RFI problem and presented formulas for approximately characterizing the fields of the DSN reflector antennas in the far (Fraunhofer) and mid (Fresnel) zones. More work is needed to produce simple closed-form theoretical pattern models for the middle as well as the near field regions. These consider the effects of surface tolerance and other irregularities of the antennas, and shall be addressed in a future paper.

ACKNOWLEDGMENT

The research described in this paper was carried out at the Jet Propulsion Laboratory, California Institute of Technology, under a contract with the National Aeronautics and Space Administration. The authors appreciate the support and helpful suggestions of Mr. Miles Sue and Dr. Ted Peng of JPL throughout the course of this research.

REFERENCES

[1] John W. Sherman, "Properties of Foucsed Apertures in the Fresnel Region," IRE Transactions on Antennas and Propagation, July 1962

[2] R. S. Wehner,"Limitations of Focused Aperture Antenna," The RAND corp., Santa Monica, Calif., Res. Memo. RM-262, U.S. Air Force Project Rand; October, 1949.

[3] A. Papoulis, Systems and Transforms with Applications in Optics, pp. 171-174, New York: McGraw-Hill, 1968

[4] Vahraz Jamnejad, "Low Side-lobe Spacecraft Antenna Pattern Study for Fixed Satellite Service (FSS) Applications," Internal JPL Document IOM 3365.036, Sep. 1987

BIOGRAPHY

Vahraz Jamnejad *is a principal engineer at the Jet Propulsion Laboratory, California Institute of Technology. He received his M.S. and Ph.D. in electrical engineering from the University of Illinois at Urbana-Champaign, specializing in electromagnetics and antennas. At JPL, he has been engaged in research and software and hardware development in various areas of spacecraft antenna technology and satellite communication systems. Among other things, he has been involved in the study, design, and development of ground and spacecraft antennas for future generations of Land Mobile Satellite Systems at L band, Personal Access Satellite Systems at K/Ka band, as well as feed arrays and reflectors for future planetary missions. His latest work on communication satellite systems involved the development of ground mobile antennas for K/Ka band mobile terminal, for use with ACTS satellite system. In the past few years, he has been active in research in parallel computational electromagnetics as well as in developing antennas for MARS sample return orbiter. More recently he has studied the applicability of large arrays of small aperture reflector antennas for the NASA Deep Space Network, and is presently active in the design of a prototype array for this application. Over the years, he has received many US patents and NASA certificates of recognition.*

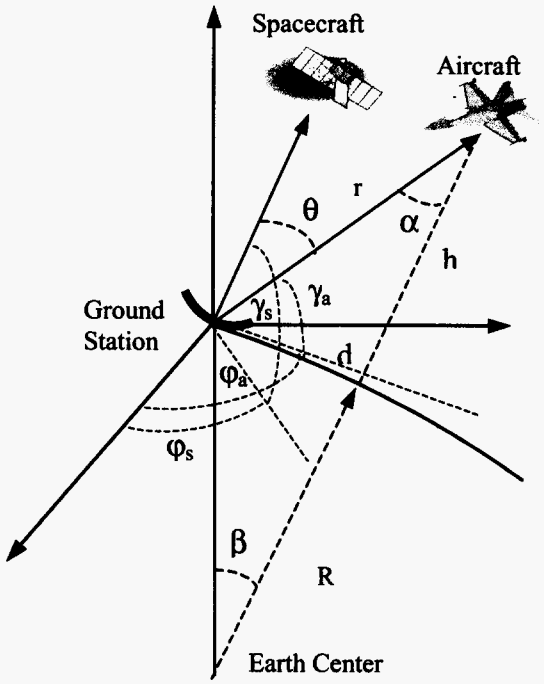

Figure 1. Geometry of the RFI problem

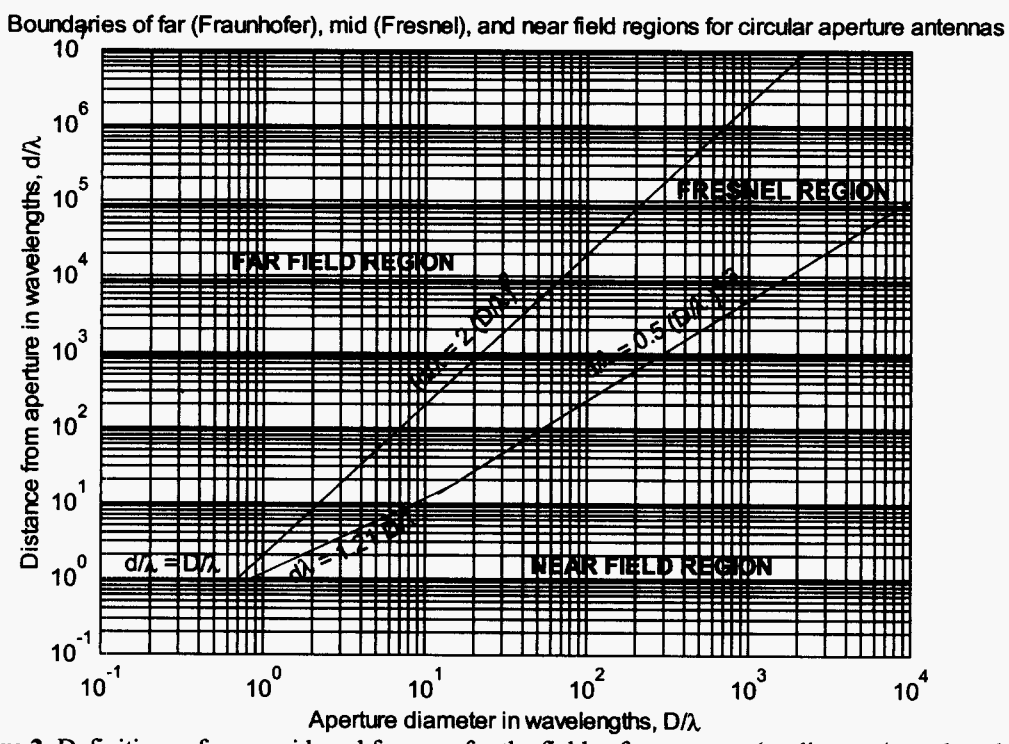

Figure 2. Definitions of near, mid, and far zone for the fields of an antenna (vs distance/wavelength)

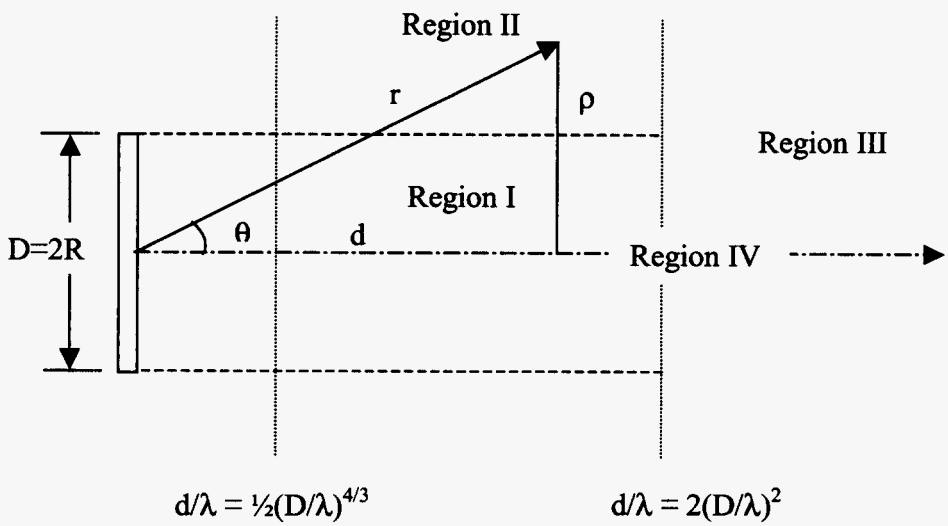

Figure 3. Geometry for defining various computation regions

Table 1. DSN antennas of interest with the applicable frequencies and transmitted power capabilities

Antenna	Band		Receive (Down-link) Frequency, GHz	Transmit (Up-link) Frequency (GHz)	Transmit power (kw)
70 meter	S-band	Near Earth	2.020-2.110	2.200-2.290	500
		Deep space	2.110-2.120	2.290-2.300	
	X-band	Deep space	8.400-8.450	7.145-7.190	20
		Near Earth	8.450-8.500	7.190-7235	500
		radar	8.500-8.565		
		VLBI	8.200-8.600		
	Ka-band		31.8-32.3 (32.050)	34.2-34.7 (34.450)	?
34 meter	S-band	Near Earth	2.020-2.110	2.200-2.290	?
		Deep space	2.110-2.120	2.290-2.300	
	X-band	Deep space	8.400-8.450	7.145-7.190	4
		Near Earth	8.450-8.500	7.190-7235	20
		radar	8.500-8.565		
		VLBI	8.200-8.600		
	Ka-band		31.8-32.3 (32.050)	34.2-34.7 (34.450)	0.8

Table 2. Near-to-mid field and mid-to-far field boundary distances of DSN antennas at differenct frequencies of operation

Band	Mode	Freq. (GHz)	Wavelength (m)	Antenna Diameter (m)			
				70		34	
				Mid > (m)	Far > (km)	Mid > (m)	Far > (km)
S-band	Transmit	2.110	0.14208	276	69	106	16
	Receive	2.290	0.13091	284	75	108	18
X-band	Transmit	7.190	0.04170	416	235	159	55
	Receive	8.450	0.03548	439	276	168	65
Ka-band	Transmit	34.450	0.00870	701	1126	268	266
	Receive	32.050	0.00935	685	1048	261	247

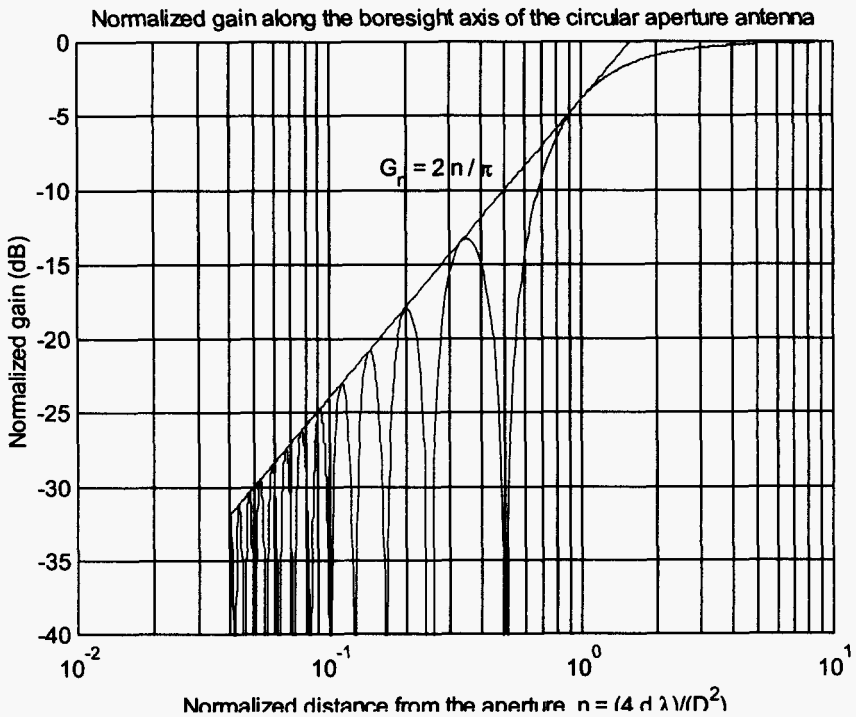

Figure 4. Normalized gain along the center axis of the aperture antenna

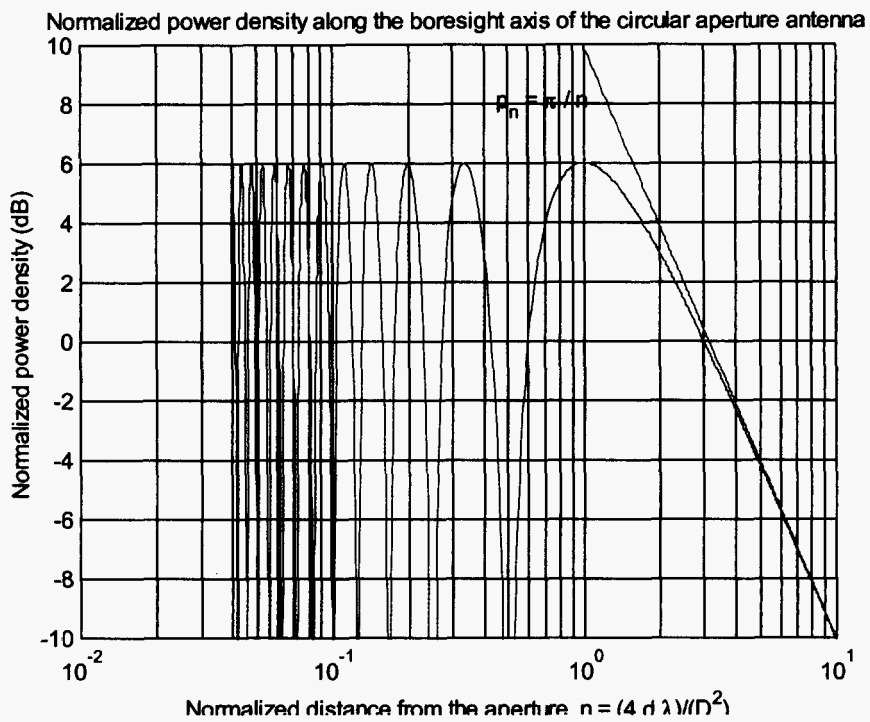

Figure 5. Normalized power density along the center axis of the aperture antenna

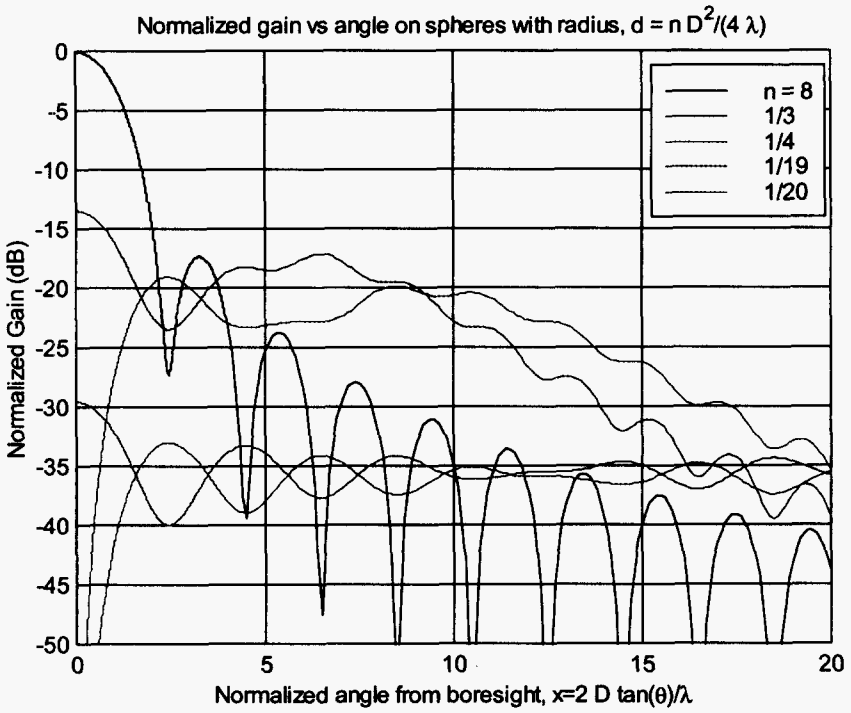

Figure 6. Normalized gain on a sphere of radius d from the aperture, as function of normalized angle from the boresight

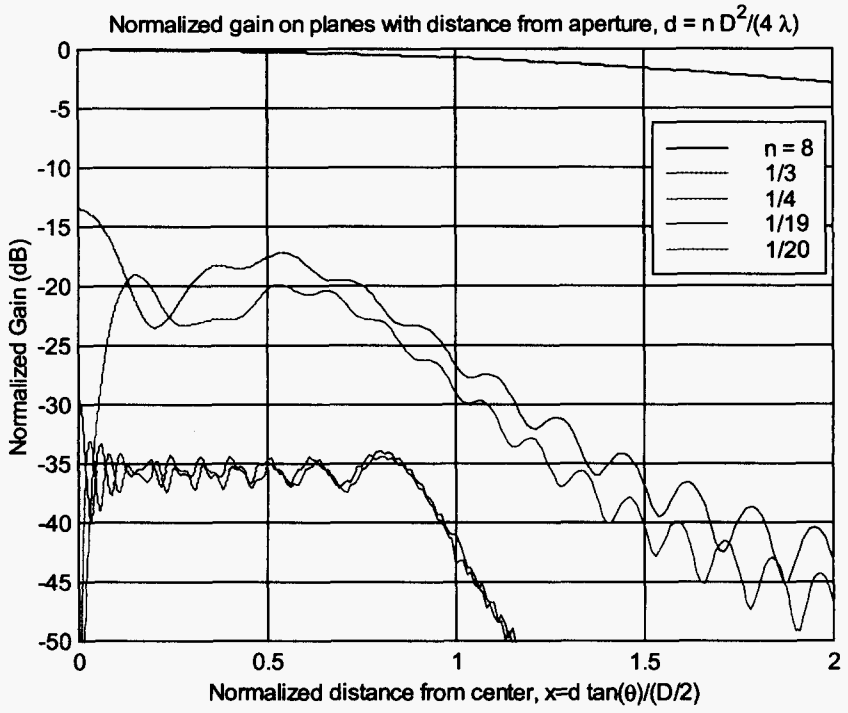

Figure 7. Normalized gain on a plane with distance d from aperture, as function of distance from axis

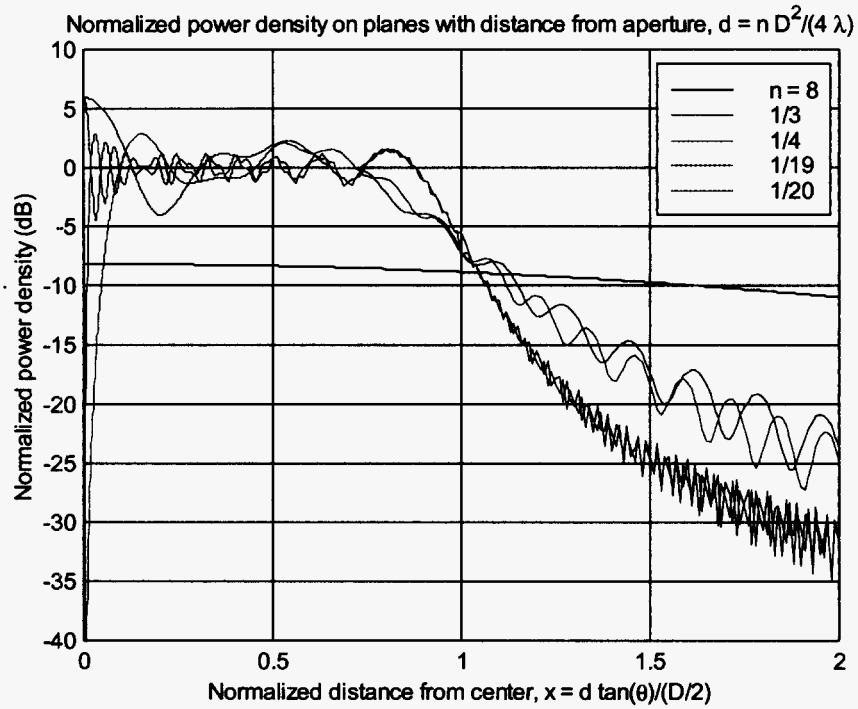

Figure 8. Normalized power density on a plane with a distance d from aperture, as function of distance from axis

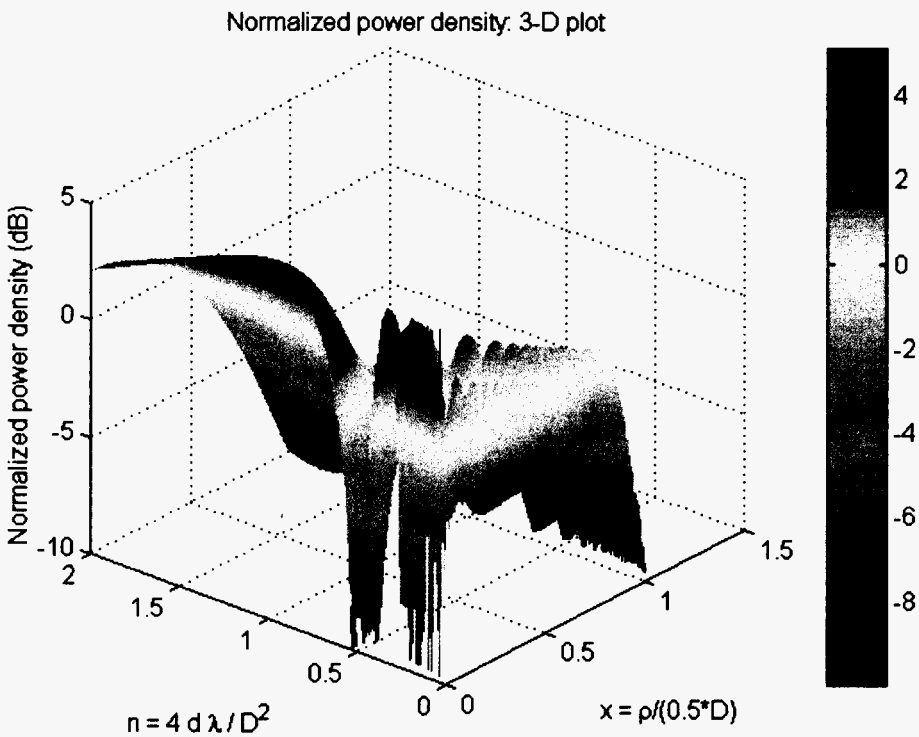

Figure 9. A 3-D plot of normalized power density (dB) of an aperture antenna

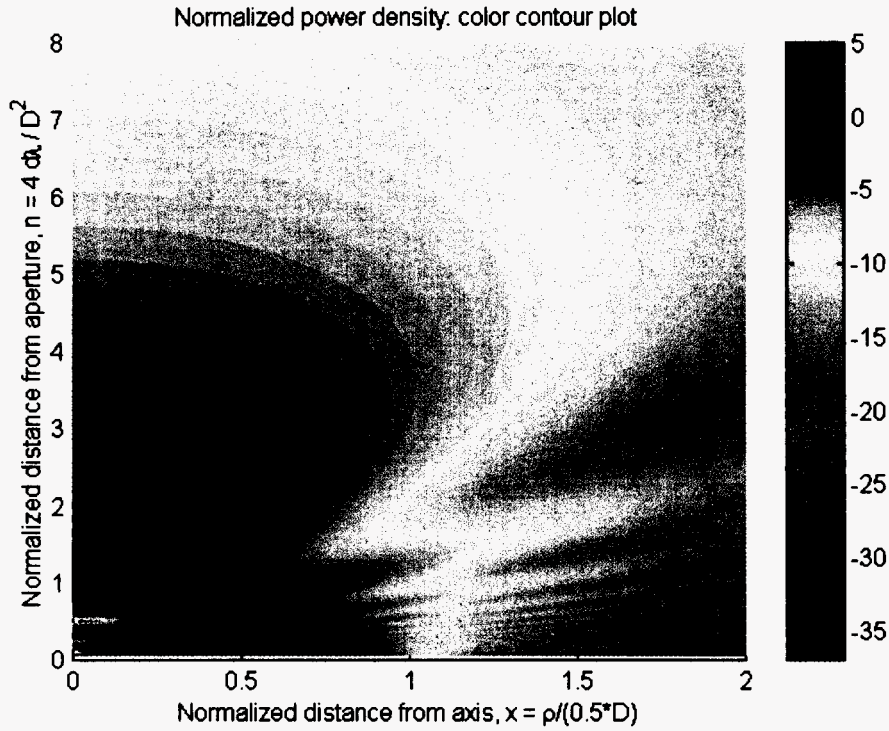

Figure 10. Color contour plot of normalized power density (dB) of an aperture antenna

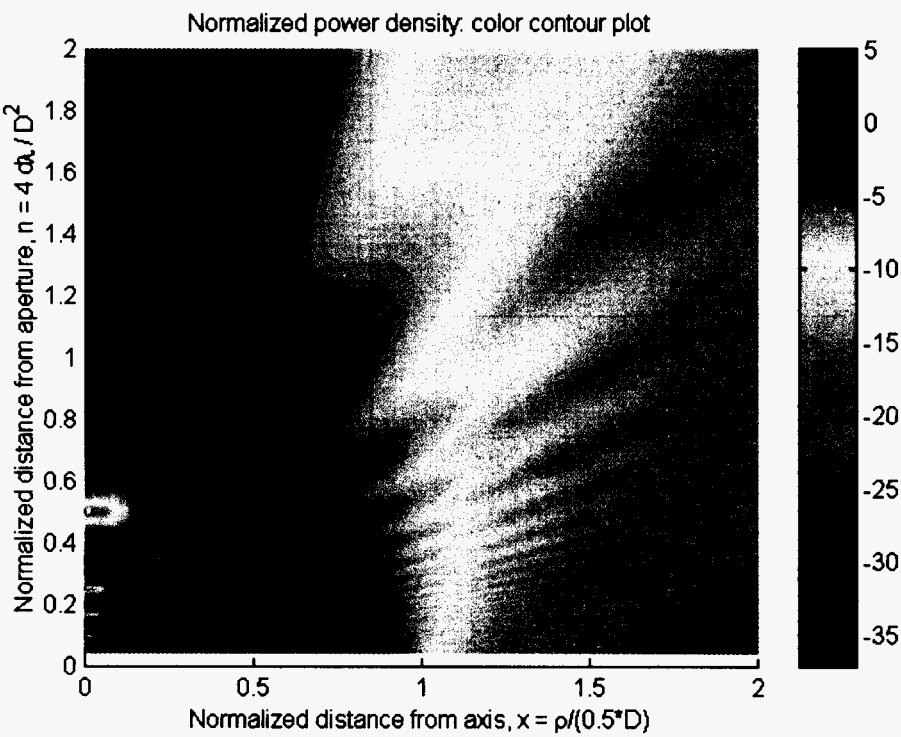

Figure 11. Color contour plot of normalized power density (dB) of an aperture antenna (expanded scale)